Outdoor Organic Photovoltaic module characteristics; benchmarking against other PV technologies for performance, calculation of Ross coefficient and outdoor stability monitoring

Bristow, Noel; Kettle, Jeffrey

Solar Energy Materials and Solar Cells

DOI:
10.1016/j.solmat.2017.10.008

Published: 01/02/2018

Peer reviewed version

Outdoor Organic Photovoltaic module characteristics; benchmarking against other PV technologies for performance, calculation of Ross coefficient and outdoor stability monitoring

N. Bristow, J. Kettle*

School of Electronic Engineering, Bangor University, Dean St., Bangor, Gwynedd, LL57 1UT, Wales, UK; email; j.kettle@bangor.ac.uk

Abstract

A comparison of performance parameters for first, second and third generation PV technologies has been conducted. Organic photovoltaic (OPV) modules displayed markedly different outdoor performance characteristics to other PV technologies owing to the positive temperature coefficient, lower thermal mass and response under low light conditions. The linear relationship between irradiance and module temperature rise above ambient is studied, leading to calculation of values for the Ross coefficient for OPV modules. OPVs are shown to possess a lower Ross coefficient than poly-Si, due to the lower absorption of infrared radiation. The effect of wind speed on the Ross coefficient is also investigated, showing the effect that module structure has upon outdoor PV performance, with the OPV module cooling quicker under windy conditions than the poly-Si due to a lower thermal mass. A long term stability study on OPV modules with a silver nanowire-zinc oxide (AgNW-ZnO) composite front electrode has showed two phases of degradation: a short initial burn-in with significant drops in performance; followed by stabilisation and degradation progressing at a much slower rate. During the burn-in period the modules showed diurnal reversible degradation in the short circuit current (I_{SC}), whereas open circuit voltage (V_{OC}) and fill factor (FF) show a steady decline. The reversible degradation is assumed to be related to the desorption of oxygen from the ZnO layer during the day due to UV excitation, leading to an increase in trap formation and a drop in current generation capacity, followed by re-adsorption of the oxygen overnight.

Keywords

Organic photovoltaics, OPV, Outdoor performance, Reliability, Ross coefficient

Highlights

- Performance of OPVs benchmarked against other technologies
- Ross coefficient reported for OPV modules
- Reversible degradation observed during “burn-in” stage

1. Introduction

Globally, wind and solar are the fastest growing sources of electricity and are now technologically mature and affordable, with the cost of utility-scale solar PV dropping by two thirds

between 2010 and 2015 [1]. In 2015 first generation silicon-based PV accounted for 93% of global production and the other 7% was from second generation thin film technologies [2]. The third generation of PV covers a much broader range of technologies, from high efficiency multi-junction (tandem) cells and concentrated PV, through to the emerging technologies of organic photovoltaics (OPVs), dye-sensitised solar cell (DSSC), perovskite and quantum dots [3,4]. The emerging technologies are looking to reduce costs by using non-toxic, abundant materials and cheap processing methods.

Research into OPVs has grown exponentially over the last decade as OPVs provide the potential for low cost and solution-based production, on flexible substrates, and at lower temperatures than silicon cells, thus reducing the embodied energy. At present OPVs lag far behind silicon based solar cells in terms of power conversion efficiency (PCE), cost (in terms of £/W_P) and lifetime. PCEs of best performing OPVs have exceeded 10% in recent years, with Toshiba recording record breaking modules (8.7%, area: 802 cm^2) and mini-modules (9.7%, area: 26 cm^2) [5]. In early 2016, Heliatek achieved a PCE of 13.2% for a multi-junction OPV device [6].

In order for these emerging PV technologies to become commercially viable it is important that it is understood how they perform under real world conditions. Research into OPVs has been beset by the problems of scalability. A meta analysis by Jørgensen et al. of about 9000 research papers on OPVs published before January 2012 provided some important insights into the current state of OPV research, including the fact that the vast majority of devices reported on were very small laboratory scale devices, 86% having an active area of 0.2 cm^2 or less [7]. Scalability has problems because, as devices get larger, the higher sheet resistivity of indium tin oxide (ITO) leads to drops in PCE [8]. Furthermore, small devices are difficult to measure outdoors with high accuracy, as the currents involved are small (nA), especially at lower irradiances, and require the use of specialist test equipment, which has impeded studies on outdoor testing.

In order to standardise the testing of OPV devices the International Summit on OPV Stability (ISOS) has published detailed protocols for measuring OPV devices, covering shelf life testing, outdoor monitoring, laboratory weathering and thermal cycling, which has enabled different laboratories to perform useful and meaningful outdoor testing [9]. One of the earliest outdoor studies on OPVs was performed by Katz et al. who published a study of outdoor degradation [10]. Many of these outdoor studies have concentrated on the importance of encapsulation, as ingress of water and oxygen, combined with UV irradiance, lead to photo-oxidation and degradation [11–13]. A study by the authors in 2015 examined the diurnal performance of OPV modules, as well as looking at its dependence on temperature and irradiation, building on work by Katz et al., Riedel et al. and Tromholt et al. [14–17]. These showed that PCE, I_{SC} and FF have positive temperature dependencies and V_{OC} has a negative temperature dependence. I_{SC} was shown to have a linear dependence on irradiance, whereas V_{OC} had a logarithmic dependence. Research by Zhang et al. has shown stability of over 1 year is possible with the right encapsulation, particularly in the vicinity of the electrical contacts [18].

In this work, a comparison of performance parameters as a function of irradiance for different PV technologies is presented, allowing a comparison of performance between first, second and third generation PV technologies. Furthermore, the dependence of module temperature rise above ambient as a function of irradiance is analysed for both silicon and OPV modules, leading to calculated values for the Ross coefficient. The effect of wind speed on the Ross coefficient is also examined. Stability studies on OPV modules are also presented showing that long-term stability is achievable, although performance is inhibited by a temporary reversible degradation during the initial burn-in period.

2. Experimental

2.1 Outdoor Monitoring Setup

The outdoor monitoring was performed at the School of Electronic Engineering, Bangor, Gwynedd (53.23°N 4.13°W), which has an altitude of 40 m above sea level and is located 500 m from the Menai Strait. The UK is classified as Oceanic (Cfb) under the Köppen-Geiger climate classification. Long term climatic averages are 14°C during summer and 4.7°C during the winter. The humidity levels are similar all year, with an average mean of 79%, an average maximum of 90%, and an average minimum of 61% in summer and 65% in winter. UV indices are very different, with an average mean of 1.07 in the summer (average maximum of 5.45) and 0.43 in the winter (average maximum of 2.38).

The outdoor monitoring system at Bangor University is located on the roof of the School of Electronic Engineering (Figure 1). The measurement system conforms to ISOS-O-2 outdoor measuring protocol [9]. It comprises two OPV module mounting racks, each of which can be independently adjusted for inclination. OPV modules are attached on raised studs to allow free air flow behind the modules. Two 8-channel multiplexers are each connected to separate source measure units (SMU) (supplied by Botest Systems GmbH), allowing two sets of up to eight modules to be monitored synchronously. Two silicon irradiance sensors (supplied by IMT Solar) are used to measure irradiance (one mounted horizontally and the other in-plane-of-array with one of the inclined OPV racks). A Davis Vantage Pro 2 weather station is used to collect meteorological data including temperature, humidity, wind speed and direction, solar radiation, UV, rainfall, and air pressure.

2.2 Modules under Test

Poly-Si: There are two 185 W_P polycrystalline silicon (poly-Si) modules (model PWSQM-48, supplied by Pure Wafer Solar Ltd.), one mounted horizontally and the other inclined at 35° and facing due south. These are each monitored by PVMS-250 measurement systems (supplied by Egnitec Ltd). Each poly-Si module has a PT100 temperature sensor, attached to its backplane, monitored by the Egnitec PVMS units.

CIS: A 36 W_P copper indium diselenide (CIS) module (model ST36, supplied by Shell) [19] is monitored by an Egnitec PVMS-250(MET) measurement system, which also monitors the two irradiance sensors and the two OPV PT100 sensors.

The Poly-Si and CIS modules are kept at maximum power point (MPP) in between periodic current-voltage (IV) sweeps (once every minute). Current and voltage at the maximum power point (I_{MPP}, V_{MPP}) and PT100 measurements are taken every 15 s.

DSSC: A dye sensitised solar cell (DSSC) was supplied by SolarPrint, Dublin. SolarPrint specialised in manufacturing DSSCs for indoor use using an electrolyte paste composed of carbon nanotubes [20]. This was mounted on the inclined OPV rack at 35° and monitored using one channel of the multiplexed SMU.

The OPV modules were fabricated and supplied by Technical University of Denmark (DTU) as part of their freeOPV programme [21]. The freeOPV modules are fabricated using a roll-to-roll process under ambient conditions with screen and flexographic printing, slot die coating and spray coating of the various layers [22,23]. The modules were encapsulated using flexible Amcor packaging barrier foil (PET coated with SiO_x barrier layers). The following freeOPV module types were used (see Figure 2):

OPV(AgGrid): These were the first generation of modules supplied under the freeOPV programme and are based on an inverted geometry with 8 serially connected cells [21]. The modules are fabricated on an ITO-free "Flextrode" PET substrate, consisting of an silver grid coated with PEDOT:PSS and then ZnO (acting as an electron transport layer) [23]. The active layer is slot die coated on top of the Flextrode, followed by PEDOT:PSS (acting as a hole transport layer) and finally an Ag grid. The top substrate is PET, which encapsulates the module using pressure sensitive adhesive. Finally, the modules are laser cut from the foil which seals the edges. Active area: 64.8 cm^2.

OPV(Carbon): These modules replace the front Ag grid with highly conductive PEDOT:PSS and carbon (graphite) busbars between the cells, and the back Ag grid with PEDOT:PSS and ZnO. The module consists of 16 serially connected cells [24]. The cells are very narrow (2 mm) due to the increased sheet resistivity of the electrodes. Active area: 30 cm^2.

OPV(AgNW): These modules are similar to the OPV(AgGrid) modules, but the front silver grid is replaced by a hybrid AgNW/ZnO layer [25]. Active area: 64.8 cm^2.

The multiplexed SMUs undertake repeated IV sweep measurement cycles every 10 minutes. The two SMUs run their measurements simultaneously. Each IV sweep takes between 10 and 30 seconds to complete and between IV sweeps the OPV modules are kept at V_{OC}. The data from each source (weather station, SMUs) was loaded into MS Access and synchronised, before being analysed using both MS Access and MS Excel.

3. Results

3.1 Benchmarking of different PV technologies

Figure 3 shows a comparison of the performance parameters for poly-Si, CIS, DSSC, OPV(AgGrid), OPV(Carbon) and OPV(AgNW) modules as a function of in-plane irradiance. As each module type has different numbers of serially connected cells with different areas, V_{OC}/cell and J_{SC}/cell have been plotted. V_{OC} has been linearly adjusted for module temperature, based on known temperature coefficients (TCs) (strongly negative for poly-Si & CIS and positive for DSSC & OPVs). All data was sourced from clear sunny days, with high levels of direct normal irradiance. For the OPV modules data was sourced from early in their monitoring campaigns, before significant degradation had occurred. Table 1 show the maximum PCE, maximum V_{OC}, the irradiance level where V_{OC} reaches 90% of its maximum and PCE, FF & J_{SC} at 800 W/m^2.

Apart from the DSSC module, all of the modules display a linear trend for J_{SC} against increasing irradiance. The DSSC module shows a linear trend until ~100 W/m^2, after which it remains linear, but increases at a reduced rate. This current limiting effect is related to the low concentration of iodine in the electrolyte, as at higher irradiances the cell is current limited by the rate of migration of I_3^- (triiodide) ions through the electrolyte and subsequent triiodide reduction rate at the counter electrode [26,27].

All modules display logarithmic V_{OC}, with DSSC possessing a maximum V_{OC} of 0.81 V/cell, poly-Si having a maximum V_{OC} of 0.61 V/cell, and CIS of 0.52 V/cell. For the OPV modules the maximum V_{OC} covers a range from 0.48 V/cell (Carbon) up to 0.57 V/cell (AgNW). These are all to expected from indoor or datasheet information. However, the rate of rise to maximum V_{OC} with increasing irradiance level varies significantly depending on the module type, with the DSSC, poly-Si and OPV(AgNW) modules reaching 90% of maximum V_{OC} at low irradiances. In the case of DSSC, 90% of maximum V_{OC} is reached at just 25 W/m^2. These modules possess very low series resistance, whereas the other modules have higher series resistance and reach 90% of maximum V_{OC} at higher irradiances, especially OPV(Carbon) at 600 W/m^2.

The poly-Si module has the highest PCE (13.6%) which is reached at an irradiance of 105 W/m^2, after which it reduces to reach 11.6% at 800 W/m^2. The changes in performance are determined primarily by the FF, which peaks at just over 0.7 before dropping off to 0.55 at higher irradiance levels. This is due to the narrowing of the bandgap and increase in saturation current with increasing temperature leading to a reduction in V_{OC}. This negative TC for V_{OC} dominates over the slightly positive TC for I_{SC}, leading to the drop in FF at higher irradiances [28]. The CIS module PCE reaches a maximum of 6.7% at ~500 W/m^2 and then only reduces very slightly with increasing irradiance. CIS modules react to increasing temperature in a similar manner to poly-Si, but the magnitude of the negative TC for V_{OC} is less, so the drop in PCE and FF is only slight [29].

The OPV modules show very different profiles for PCE changes as a function of irradiance level, reaching their maxima at much higher irradiances (600-800 W/m^2) and then staying relatively constant thereafter, whereas FF starts at low values and steadily increases with increasing irradiance. However, the three modules show markedly different performance, with the subsequent generations of fabrication materials showing improved performance with improved processing methods, with maximum PCE increasing from just 0.69% for the OPV(AgGrid) to 2.5% for the OPV(AgNW). The OPV(Carbon) module has particularly poor V_{OC} performance, due to the use of carbon as an electrode, indicating a poor work function match. The use of carbon in the electrode also leads to a higher series resistance, leading to lower FF (maximum of 0.35). The OPV(AgNW) module in comparison has a fast rise in its V_{OC} and a maximum FF of 0.6, which falls to only 0.53 at maximum irradiances.

In OPVs, charge carrier transport in polymers is governed by carrier hopping and is therefore thermally assisted, which means that mobility and charge-carrier transport should improve with increasing temperature [30]. In addition, temperature increases will also lead to more efficient dissociation of electrons and holes [31]. FF has a positive TC, attributed to a decrease in series resistance with increasing temperature, whereas shunt resistance remains relatively unchanged [16]. Overall, this leads to strongly positive TCs for I_{SC} and FF and only a weak negative TC for V_{OC}, which leads to a positive TC for PCE. These results highlight the improvements being made in the fabrication techniques and materials used in these OPV modules from DTU, leading to improved light capture (increased Jsc) and reduced series resistance (higher FF).

3.2 Ross Coefficient for OPVs

Examination of Figure 4a shows the linear relationship between T_{DELTA} (the temperature rise of the module above ambient) and irradiance for an OPV and a poly-Si module, defined by Equation (1), where *G* is irradiance and *k* is the slope, known as the Ross coefficient [32].

$$\boldsymbol{T_{DELTA} = T_{module} - T_{ambient} = kG} \quad \textbf{(1)}$$

The values obtained for the Ross coefficient at wind speeds below 0.5 m/s are: OPV=0.027 K.m^2/W and poly-Si=0.028 K.m^2/W. The latter is in line with expected values for freestanding PV modules [33]. The poly-Si module has a slightly higher coefficient than the OPV module and this is thought to be due to the ability of the modules to absorb infrared radiation up to 1100 nm, compared to 650 nm for the OPV modules (P3HT:$PC_{61}BM$ [34,35].

Figure 4b shows the effect of wind speed on the Ross coefficient. Both module types drop to a constant at wind speeds above about 5 m/s, with the poly-Si reducing to 0.015 K.m^2/W and the OPV to 0.011 K.m^2/W. The primary reason for this difference is related to the differences in thermal mass; the OPV module (PET-cell-PET) possesses a much lower thermal mass than the poly-Si module (glass-cell-tedlar), due to the thinness of the substrate, and therefore the OPV modules have a faster rate of cooling with increasing wind speed [33,36].

3.3 Improving Stability using Silver Nanowire Front Electrodes

When outdoor monitoring has been conducted on OPV(AgGrid) modules, the degradation was found to degrade with 3 months of operation [14]. Rapid degradation was observed in these mini-modules due to oxygen and water ingress at the contacts and at the edges due to the high perimeter-to-edge ratio. Here we examine data for the OPV(AgNW) modules, which was monitored outdoors from 16/04/2015 till 17/07/2015. The primary difference between this module and the OPV(AgGrid) modules is that the front electrode has been altered; a composite electrode of AgNW and ZnO has been used in the OPV(AgNW) modules. The ZnO thickness has to be increased for optimal processing and therefore absorbs more UV irradiation [37].

Figure 5 shows the degradation of the performance parameters selected at irradiances of 600±15 W/m^2 and 1000±15 W/m^2. The PCE curves show a rapid deterioration during burn-in over the first week or so, dropping from 2.5% to just below 2% (T_{80} = 6 days). This loss of PCE mainly comes from a drop in FF as well as a very slight drop in V_{OC}. Once the module reaches stabilisation it is followed by a much slower degradation for the remainder of the outdoor monitoring; characteristic behaviour for these types of modules [38]. The PCE stabilises at about 1.8% and maintains this for the rest of the monitoring period and I_{SC} increases very slightly over the course of the monitoring. FF and V_{OC} degrade very slowly over the same period. It is clear that using the AgNW/ZnO composite electrode greatly enhances the stability in an outdoor environment with less photo-bleaching occurring at the edges and contacts, supporting the view that the greater ZnO thickness reduces UV penetration into the active layer.

To understand performance changes in more detail, PCE as a function of irradiance was plotted for a sunny day early on in the monitoring campaign (Figure 6a). The evolution of PCE during the morning and afternoon has been highlighted and a drop in performance is evident in the afternoon. As it was a clear sunny day, irradiance followed the expected diurnal trend, with a steady increase during the morning and decrease in the afternoon/evening (see inset in Figure 6a). OPV module temperature is normally greater in the afternoon on sunny days due to radiant heating [14], which indicates this drop is not due to a temperature difference. Furthermore, this reversible degradation was not observed on cloudy days, with low levels of irradiance and UV. Examination of data later in the monitoring period, after stabilisation had been reached, showed that this morning/afternoon split no longer occurred.

Figure 6b shows morning and afternoon IV curves on two consecutive sunny days (all selected where irradiance was at a similar level: 205±5 W/m^2), with the current linearly adjusted to 1000 W/m^2 and Table 2 shows the performance parameters obtained from this data. It can be seen that V_{OC} and FF both reduce over the course of the day and then improve (but not fully recover) overnight. In contrast, I_{SC} also reduces over the course of the day, but returns nearly to its original value by the next morning. These trends are repeated over the course of the next day. We suppose this reversible degradation is caused by the desorption of oxygen from the ZnO layer during the day due to UV excitation [39]. This de-doping causes the formation of traps, which lead to a drop in the current generation capability of the

cell. During periods of darkness the oxygen is re-adsorbed by the ZnO leading to a recovery. At the same time there is non-reversible photo-chemical degradation during the initial burn-in period, which causes an increase in the series resistance, which leads to the drop in FF and to a lesser extent in V_{OC} [40].

Conclusion/Summary

Comparison of the performance parameters as a function of irradiance for several different module types is reported. OPV modules displayed markedly different outdoor performance characteristics to other PV technologies. Detailed analysis of the poly-Si and OPV modules show a linear relationship between temperature rise and irradiance for both poly-Si and OPV modules and this data is used to calculate values for the Ross coefficient of 0.028 $K.m^2/W$ for poly-Si and 0.027 $K.m^2/W$ for OPV. Analysis of the effect of wind speed on the Ross coefficient highlights the impact of different materials used in the fabrication of the modules. The higher thermal mass of the poly-Si module leads to less loss at higher wind speeds than the lightweight flexible OPV module, although both show similar characteristics, dropping to steady values at wind speeds above 0.5 m/s. Improved stability was observed from OPV(AgNW) modules, however, the stability results showed two prominent phases of degradation: a short initial burn-in with significant drops in PCE and FF; before stabilising and degrading at a lower rate. During the burn-in period the modules showed diurnal reversible degradation, with I_{SC} dropping over the course of the day, but restoring to its original value by next morning, whereupon it repeats the same pattern. By comparison FF and V_{OC} showed a steady non-reversible degradation with only a very slight recovery overnight. The reversible degradation is caused by the desorption of oxygen from the ZnO layer during the day due to UV excitation, leading to an increase in trap formation and a drop in current generation capacity, followed by re-adsorption of the oxygen overnight.

Acknowledgements

The authors would particularly like to thank Morten Madsen and Frederik Krebs of the Technical University of Denmark for their advice, support and for supplying the OPV modules through the generous “freeOPV programme”. The work was supported by the Solar Photovoltaic Academic Research Consortium II (SPARC II) project, gratefully funded by WEFO.

References

[1] International Energy Agency, Tracking Clean Energy Progress 2016, Int. Energy Agency Books Online. (2016). http://www.iea.org/publications/freepublications/publication/TrackingCleanEnergyProgress2016.pdf.

[2] Fraunhofer Institute for Solar Energy Systems, Photovoltaics Report, (2016).

https://www.ise.fraunhofer.de/en/downloads-englisch/pdf-files-englisch/photovoltaics-report-slides.pdf.

[3] G.F. Brown, J. Wu, Third generation photovoltaics, Laser Photonics Rev. 3 (2009) 394–405. doi:10.1002/lpor.200810039.

[4] M.A. Green, Third generation photovoltaics: Assessment of progress over the last decade, 34th IEEE Photovolt. Spec. Conf. (2009) 000146–000149. doi:10.1109/PVSC.2009.5411708.

[5] M.A. Green, K. Emery, Y. Hishikawa, W. Warta, E.D. Dunlop, Solar cell efficiency tables (version 48), Prog. Photovolt. Res. Appl. 24 (2016) 905–913. doi:10.1002/pip.2788.

[6] Heliatek Gmbh, Heliatek sets new OPV world record efficiency of 13.2%, (2016). http://www.heliatek.com/en/press/press-releases/details/heliatek-sets-new-organic-photovoltaic-world-record-efficiency-of-13-2 (accessed June 25, 2016).

[7] M. Jørgensen, J.E. Carlé, R.R. Søndergaard, M. Lauritzen, N.A. Dagnæs-Hansen, S.L. Byskov, T.R. Andersen, T.T. Larsen-Olsen, A.P.L. Böttiger, B. Andreasen, L. Fu, L. Zuo, Y. Liu, E. Bundgaard, X. Zhan, H. Chen, F.C. Krebs, The state of organic solar cells — A meta analysis, Sol. Energy Mater. Sol. Cells. 119 (2013) 84–93. doi:10.1016/j.solmat.2013.05.034.

[8] J.D. Servaites, S. Yeganeh, T.J. Marks, M.A. Ratner, Efficiency Enhancement in Organic Photovoltaic Cells: Consequences of Optimizing Series Resistance, Adv. Funct. Mater. 20 (2010) 97–104. doi:10.1002/adfm.200901107.

[9] M.O. Reese, S.A. Gevorgyan, M. Jørgensen, E. Bundgaard, S.R. Kurtz, D.S. Ginley, D.C. Olson, M.T. Lloyd, P. Morvillo, E.A. Katz, A. Elschner, O. Haillant, T.R. Currier, V. Shrotriya, M. Hermenau, M. Riede, K. R. Kirov, G. Trimmel, T. Rath, O. Inganäs, F. Zhang, M. Andersson, K. Tvingstedt, M. Lira-Cantu, D. Laird, C. McGuiness, S. (Jimmy) Gowrisanker, M. Pannone, M. Xiao, J. Hauch, R. Steim, D.M. DeLongchamp, R. Rösch, H. Hoppe, N. Espinosa, A. Urbina, G. Yaman-Uzunoglu, J.-B. Bonekamp, A.J.J.M. van Breemen, C. Girotto, E. Voroshazi, F.C. Krebs, Consensus stability testing protocols for organic photovoltaic materials and devices, Sol. Energy Mater. Sol. Cells. 95 (2011) 1253–1267. doi:10.1016/j.solmat.2011.01.036.

[10] E.A. Katz, S. Gevorgyan, M.S. Orynbayev, F.C. Krebs, Out-door testing and long-term stability of plastic solar cells, Eur. Phys. J. Appl. Phys. 36 (2006) 307–311. doi:10.1051/epjap.

[11] J.A. Hauch, P. Schilinsky, S.A. Choulis, R. Childers, M. Biele, C.J. Brabec, Flexible organic P3HT : PCBM bulk-heterojunction modules with more than 1 year outdoor lifetime, Sol. Energy Mater. Sol. Cells. 92 (2008) 727–731. doi:10.1016/j.solmat.2008.01.004.

[12] D. Angmo, F.C. Krebs, Over 2 Years of Outdoor Operational and Storage Stability of ITO-Free, Fully Roll-to-Roll Fabricated Polymer Solar Cell Modules, Energy Technol. 3 (2015) 774–783. doi:10.1002/ente.201500086.

[13] B. Roth, G.A. dos Reis Benatto, M. Corazza, R.R. Søndergaard, S.A. Gevorgyan, M. Jørgensen,

F.C. Krebs, The Critical Choice of PEDOT:PSS Additives for Long Term Stability of Roll-to-Roll Processed OPVs, Adv. Energy Mater. 5 (2015). doi:10.1002/aenm.201401912.

[14] N. Bristow, J. Kettle, Outdoor performance of organic photovoltaics: Diurnal analysis, dependence on temperature, irradiance, and degradation, J. Renew. Sustain. Energy. 7 (2015) 13111. doi:10.1063/1.4906915.

[15] E.A. Katz, D. Faiman, S.M. Tuladhar, J.M. Kroon, M.M. Wienk, T. Fromherz, F. Padinger, C.J. Brabec, N.S. Sariciftci, Temperature dependence for the photovoltaic device parameters of polymer-fullerene solar cells under operating conditions, J. Appl. Phys. 90 (2001) 5343. doi:10.1063/1.1412270.

[16] I. Riedel, J. Parisi, V. Dyakonov, L. Lutsen, D. Vanderzande, J.C. Hummelen, Effect of Temperature and Illumination on the Electrical Characteristics of Polymer–Fullerene Bulk-Heterojunction Solar Cells, Adv. Funct. Mater. 14 (2004) 38–44. doi:10.1002/adfm.200304399.

[17] T. Tromholt, E.A. Katz, B. Hirsch, A. Vossier, F.C. Krebs, Effects of concentrated sunlight on organic photovoltaics, Appl. Phys. Lett. 96 (2010) 73501. doi:10.1063/1.3298742.

[18] Y. Zhang, H. Yi, A. Iraqi, J. Kingsley, A. Buckley, T. Wang, D.G. Lidzey, Comparative indoor and outdoor stability measurements of polymer based solar cells, Sci. Rep. 7 (2017) 1305. doi:10.1038/s41598-017-01505-w.

[19] Shell ST36 PV Module Specification, (n.d.). http://www.atlantasolar.com/pdf/Shell/ShellST36_USv1.pdf (accessed July 10, 2016).

[20] S.U. Lee, W.S. Choi, B. Hong, A comparative study of dye-sensitized solar cells added carbon nanotubes to electrolyte and counter electrodes, Sol. Energy Mater. Sol. Cells. 94 (2010) 680–685. doi:10.1016/j.solmat.2009.11.030.

[21] F.C. Krebs, M. Hösel, M. Corazza, B. Roth, M. V. Madsen, S.A. Gevorgyan, R.R. Søndergaard, D. Karg, M. Jørgensen, Freely available OPV - The fast way to progress, Energy Technol. 1 (2013) 378–381. doi:10.1002/ente.201300057.

[22] D. Angmo, S.A. Gevorgyan, T.T. Larsen-Olsen, R.R. Søndergaard, M. Hösel, M. Jørgensen, R. Gupta, G.U. Kulkarni, F.C. Krebs, Scalability and stability of very thin, roll-to-roll processed, large area, indium-tin-oxide free polymer solar cell modules, Org. Electron. 14 (2013) 984–994. doi:10.1016/j.orgel.2012.12.033.

[23] M. Hösel, R.R. Søndergaard, M. Jørgensen, F.C. Krebs, Fast Inline Roll-to-Roll Printing for Indium-Tin-Oxide-Free Polymer Solar Cells Using Automatic Registration, Energy Technol. 1 (2013) 102–107. doi:10.1002/ente.201200029.

[24] G.A. dos Reis Benatto, B. Roth, M. V. Madsen, M. Hösel, R.R. Søndergaard, M. Jørgensen, F.C. Krebs, Carbon: The ultimate electrode choice for widely distributed polymer solar cells, Adv. Energy Mater. 4 (2014). doi:10.1002/aenm.201400732.

[25] G.A. dos Reis Benatto, B. Roth, M. Corazza, R.R. Søndergaard, S.A. Gevorgyan, M. Jørgensen, F.C. Krebs, Roll-to-roll printed silver nanowires for increased stability of flexible ITO-free organic solar cell modules., Nanoscale. 8 (2016) 318–26. doi:10.1039/c5nr07426f.

[26] A. Hauch, A. Georg, Diffusion in the electrolyte and charge-transfer reaction at the platinum electrode in dye-sensitized solar cells, Electrochim. Acta. 46 (2001) 3457–3466. doi:10.1016/S0013-4686(01)00540-0.

[27] T. Toyoda, T. Sano, J. Nakajima, S. Doi, S. Fukumoto, A. Ito, T. Tohyama, M. Yoshida, T. Kanagawa, T. Motohiro, T. Shiga, K. Higuchi, H. Tanaka, Y. Takeda, T. Fukano, N. Katoh, A. Takeichi, K. Takechi, M. Shiozawa, Outdoor performance of large scale DSC modules, J. Photochem. Photobiol. A Chem. 164 (2004) 203–207. doi:10.1016/j.jphotochem.2003.11.022.

[28] E. Skoplaki, J.A. Palyvos, On the temperature dependence of photovoltaic module electrical performance: A review of efficiency/power correlations, Sol. Energy. 83 (2009) 614–624. doi:10.1016/j.solener.2008.10.008.

[29] V. Perraki, G. Tsolkas, Temperature dependence on the photovoltaic properties of selected thin-film modules 2 . Effect of Temperature on the I-V Characteristics of PV Modules, 2 (2013) 140–146. doi:10.11648/j.ijrse.20130204.12.

[30] G. Malliaras, R. Friend, An Organic Electronics Primer, Phys. Today. 58 (2005) 53. doi:10.1063/1.1995748.

[31] L.A. Ribeiro, W.F. Cunha, P.H.O. Neto, R. Gargano, G.M. Silva, Impurity effects and temperature influence on the exciton dissociation dynamics in conjugated polymers, Chem. Phys. Lett. 580 (2013) 108–114. doi:10.1016/j.cplett.2013.06.065.

[32] R.G. Ross, Interface design considerations for terrestrial solar cell modules, 12th IEEE Photovolt. Spec. Conf. 1 (1976).

[33] L. Maturi, G. Belluardo, D. Moser, M. Del Buono, BiPV system performance and efficiency drops: Overview on PV module temperature conditions of different module types, Energy Procedia. 48 (2014) 1311–1319. doi:10.1016/j.egypro.2014.02.148.

[34] E. Skoplaki, A.G. Boudouvis, J.A. Palyvos, A simple correlation for the operating temperature of photovoltaic modules of arbitrary mounting, Sol. Energy Mater. Sol. Cells. 92 (2008) 1393–1402. doi:10.1016/j.solmat.2008.05.016.

[35] A. Larkin, J.D. Haigh, S. Djavidnia, The effect of solar UV irradiance variations on the earth's atmosphere, Space Sci. Rev. 94 (2000) 199–214. doi:10.1023/A:1026771307057.

[36] E. Skoplaki, J.A. Palyvos, Operating temperature of photovoltaic modules: A survey of pertinent correlations, Renew. Energy. 34 (2009) 23–29. doi:10.1016/j.renene.2008.04.009.

[37] Frederik C. Krebs, private communication, 2014.

[38] M. Corazza, F.C. Krebs, S.A. Gevorgyan, Predicting, categorizing and intercomparing the lifetime of OPVs for different ageing tests, Sol. Energy Mater. Sol. Cells. 130 (2014) 99–106. doi:10.1016/j.solmat.2014.06.031.

[39] T. Tromholt, A. Manor, E.A. Katz, F.C. Krebs, Reversible degradation of inverted organic solar cells by concentrated sunlight., Nanotechnology. 22 (2011) 225401. doi:10.1088/0957-4484/22/22/225401.

[40] E. Voroshazi, B. Verreet, T. Aernouts, P. Heremans, Long-term operational lifetime and degradation analysis of P3HT:PCBM photovoltaic cells, Sol. Energy Mater. Sol. Cells. 95 (2011) 1303–1307. doi:10.1016/j.solmat.2010.09.007.

Table 1: Comparison of PV performance parameters for poly-Si, CIS, DSSC and three OPV modules.

Module Type	Maximum PCE (%)	Maximum V_{OC}/cell (V)	Irradiance at 90% of maximum V_{OC} (W/m^2)	Performance parameters @ 800 W/m^2		
				PCE (%)	**FF**	**J_{SC}/cell (mA/cm^2)**
Poly-Si	13.6	0.61	110	11.1	0.58	26.6
CIS	6.7	0.53	260	6.5	0.49	20.8
DSSC	10.0	0.81	25	0.9	0.44	2.1
OPV(AgGrid)	0.69	0.52	330	0.67	0.42	2.5
OPV(Carbon)	0.78	0.48	600	0.72	0.33	3.8
OPV(AgNW)	2.50	0.57	120	2.34	0.56	5.2

Table 2: PV performance parameters of an OPV(AgNW) module on consecutive days, comparing morning and afternoon characteristics measured at similar irradiances. Percentages in brackets show change relative to the previous measurement.

Date	Time	Irradiance (W/m^2)	$T_{Ambient}$ (°C)	I_{SC} (mA)	V_{OC} (V)	FF	PCE (%)
20/04/2015	07:16	206	8.4	12.05	4.20	0.549	2.08
	17:21	200	11.7	11.02 (-8.6%)	4.00 (-4.8%)	0.436 (-20.6%)	1.49 (-28%)
21/04/2015	07:11	204	8.8	12.28 (+12%)	4.05 (+1.3%)	0.451 (+3.3%)	1.69 (+14%)
	17:21	211	11.6	11.83 (-3.7%)	3.65 (-9.9%)	0.418 (-7.2%)	1.32 (-22%)

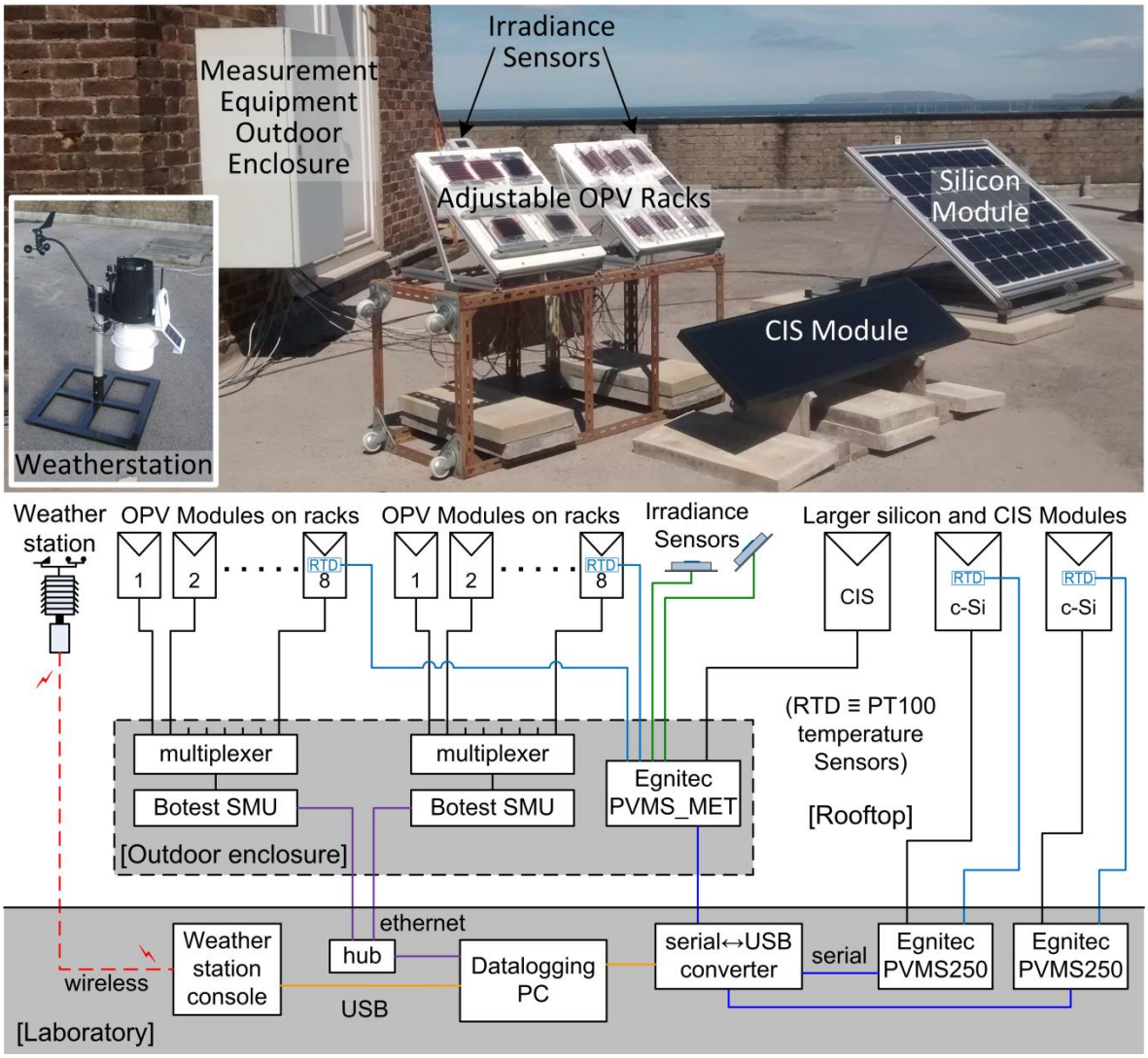

Figure 1: Photograph (top) and system schematic (bottom) of the outdoor monitoring system on the roof of the School of Electronic Engineering at Dean Street, Bangor (inset in photograph shows the wireless weather station).

a)

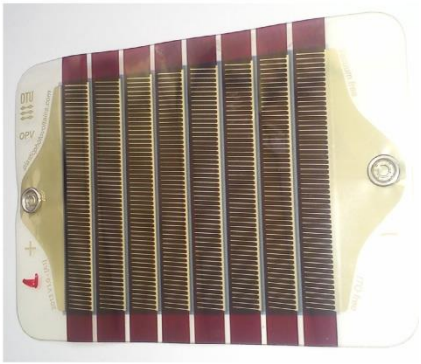

b)

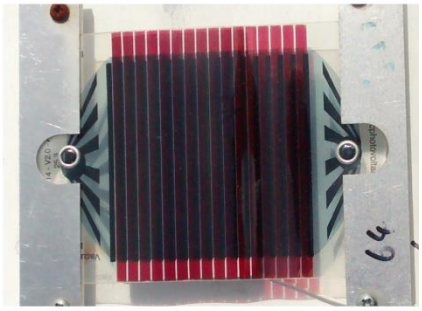

c)

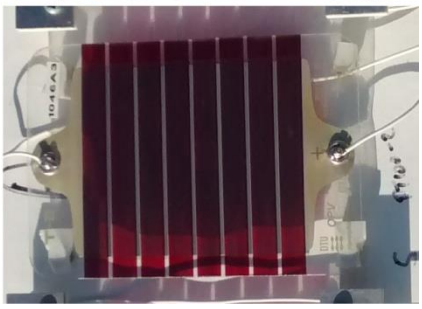

Figure 2: DTU freeOPV modules: a) OPV(AgGrid), first generation freeOPV modules with silver grid electrodes at front and rear; b) OPV(Carbon), freeOPV module with graphite busbars; and c) OPV(AgNW), freeOPV module with silver nanowire front electrode.

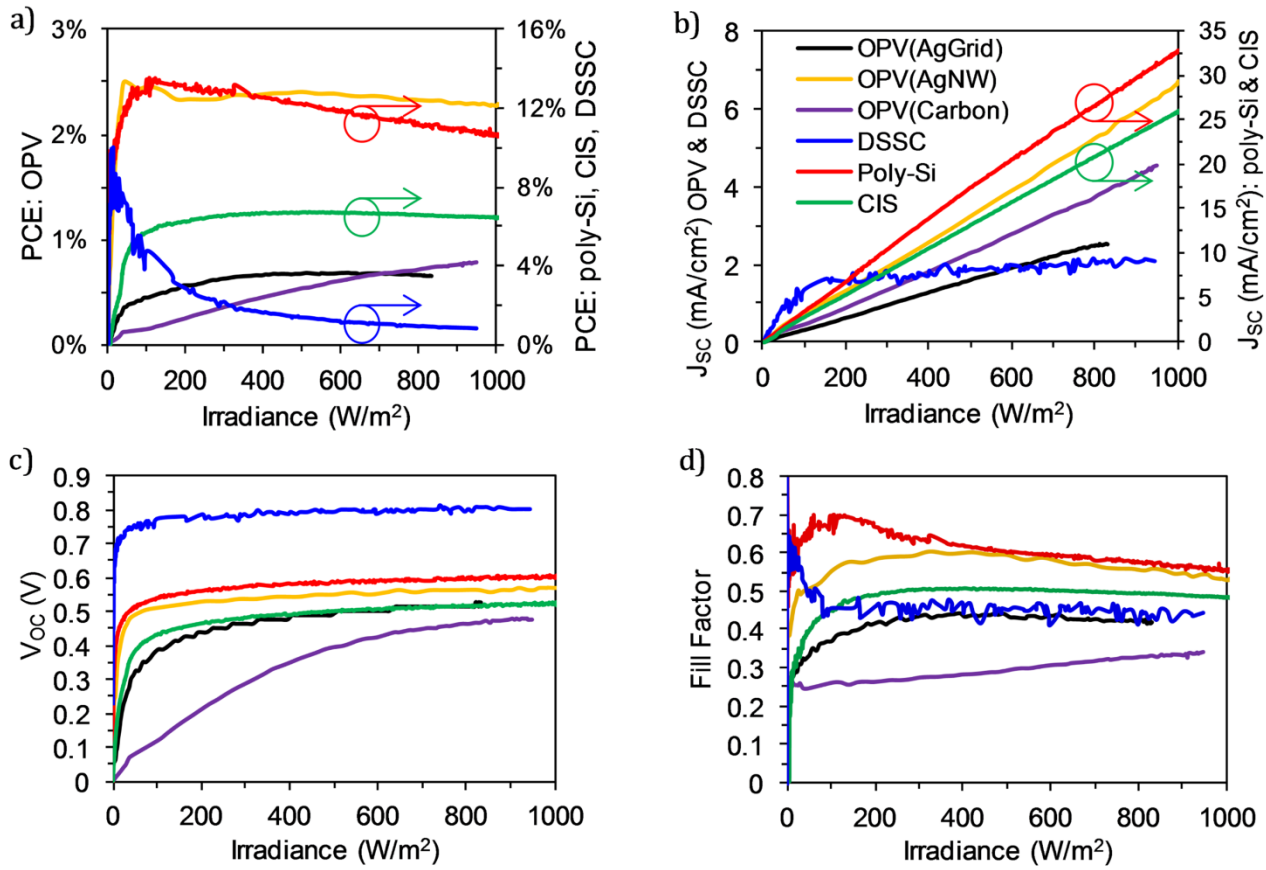

Figure 3: Comparison of performance parameters for poly-Si, CIS, DSSC and three different OPV modules: a) PCE; b) J_{SC} (per cell); c) V_{OC} (per cell); and d) FF.

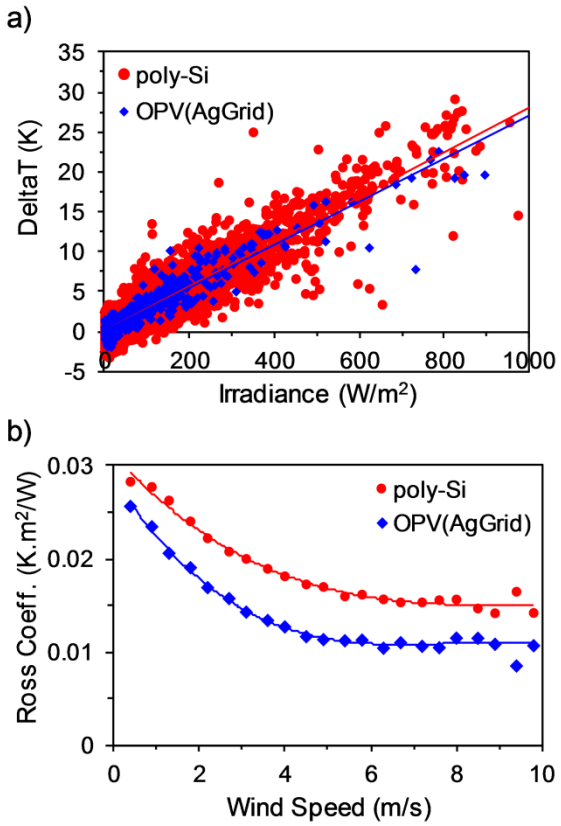

Figure 4: a) Effect of irradiance on module temperature rise above ambient (T_{DELTA}) plotted against irradiance with linear trend lines. The slope of each line is the Ross coefficient. b) Effect of wind speed on Ross coefficient.

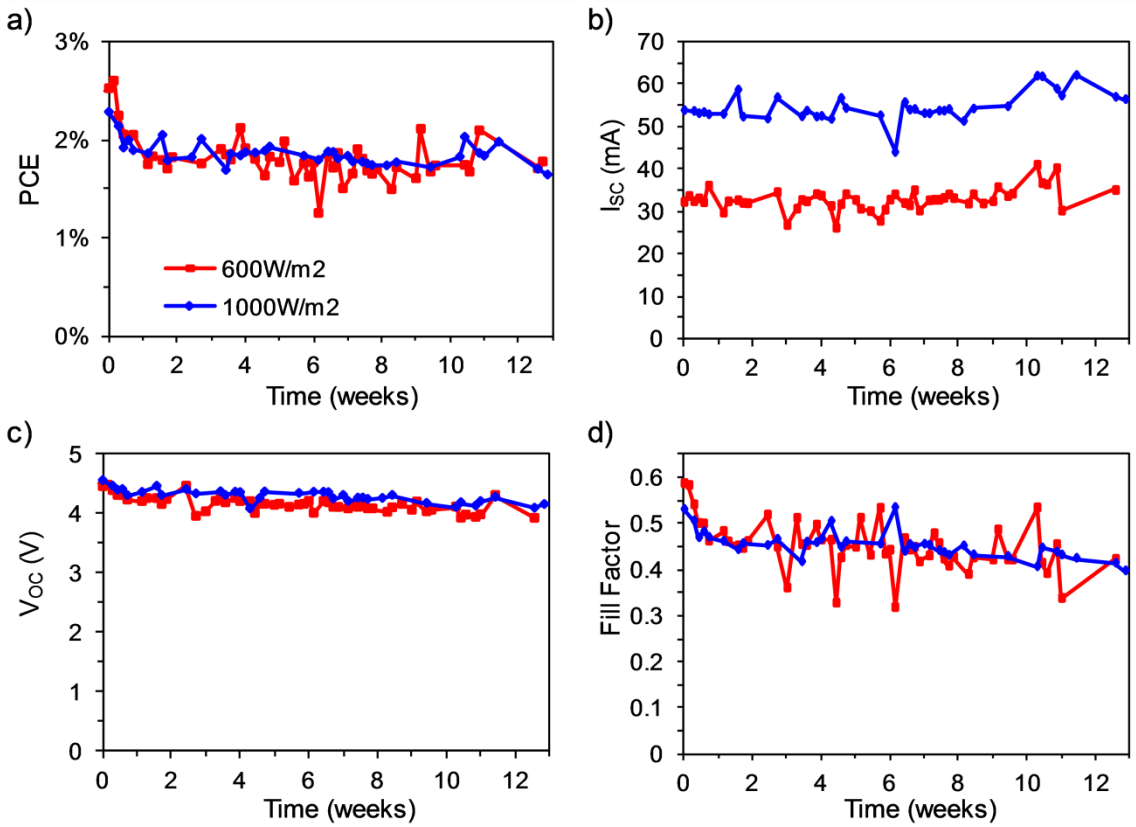

Figure 5: Degradation of OPV modules with silver nanowire front electrodes: a) PCE; b) I_{SC}; c) V_{OC}; and d) FF. Measurements were selected at two different irradiances (600±15 W/m^2 and 1000±15 W/m^2) and daily averages are plotted.

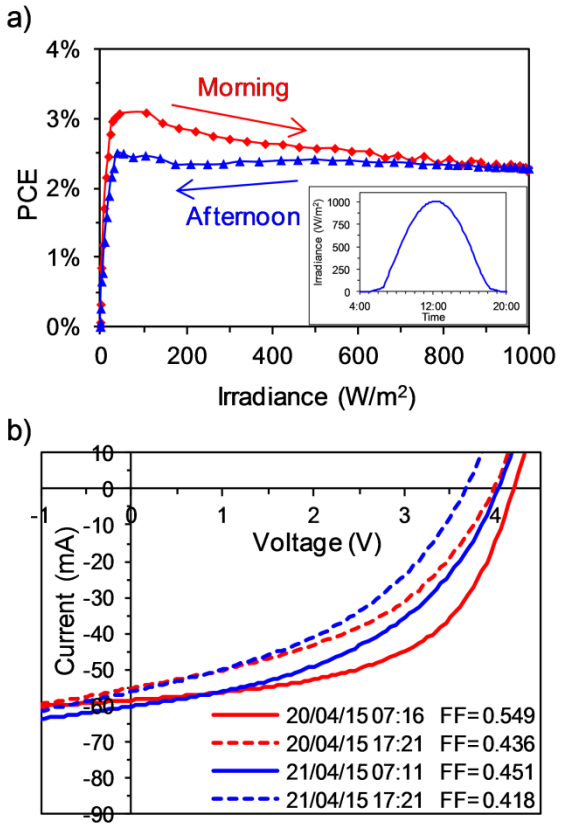

Figure 6: a) PCE plotted against irradiance on a sunny day (inset graph shows irradiance vs. time), highlighting the different pattern in the morning and afternoon; b) Comparison of morning (solid) and afternoon (dashed) IV curves on 2 consecutive sunny days [current linearly adjusted to 1000 W/m^2].